Electronic Supplementary Material (ESI) for Physical Chemistry Chemical Physics.

Supplementary Material

Vacancy defects impede the transition from peapods to diamond: a neuroevolution machine learning study

Yu Li

Shanghai Key Laboratory of Mechanics in Energy Engineering,
Shanghai Institute of Applied Mathematics and Mechanics,
Shanghai Frontier Science Center of Mechanoinformatics,
School of Mechanics and Engineering Science,
Shanghai University, Shanghai 200072, People's Republic of China

Jin-Wu Jiang*

Shanghai Key Laboratory of Mechanics in Energy Engineering,
Shanghai Institute of Applied Mathematics and Mechanics,
Shanghai Frontier Science Center of Mechanoinformatics,
School of Mechanics and Engineering Science,
Shanghai University, Shanghai 200072, People's Republic of China
Zhejiang Laboratory, Hangzhou 311100, China

Section 1

All tunable hyperparameters used in the NEP potential are displayed in Table S1. Here, r_c^R and r_c^A are the cutoff radius for radial and angular descriptor components, respectively. n_{max}^R and n_{max}^A are the Chebyshev polynomial expansion order for radial and angular descriptor components. N_{bas}^R and N_{bas}^A are the number of radial and angular basis functions. l_{max}^{3b} and l_{mas}^{4b} are three-body interation order and four-body interation order of angular descriptor components. N_{neu} is the number of neurons in the hidden layer of the neural network. λ_1 and λ_2 are the L_1 and L_2 regularization parameter. λ_e, λ_f and λ_v are the weight factors of energy, force and virial coefficients. N_{bat} is the batch size, N_{pop} is the population size in the natural evolution strategy algorithm, and N_{gen} is the maximum number of evolution generations.

Figure S1 shows a comparison of the computational performance of NEP-C models, GAP-20, and AIREBO potentials in realistic atomistic simulations. We run MD simulations for a perfect peapod array in the isothermal ensemble at 300 K for 100 steps to test the computational speed. The computational speed is measured as the product of the number of atoms and the number of steps divided by the total wall time

Table S1: Hyperparameters for the NEP-C model.

parameter	value	parameter	value
r_c^R	7 Å	r_c^A	3.5 Å
n_{max}^R	8	n_{max}^A	8
N_{bas}^R	8	N_{bas}^A	8
l_{max}^{3b}	4	l_{mas}^{4b}	2
N_{neu}	100	λ_1	0.05
λ_2	0.05	λ_e	1.0
λ_f	1.0	λ_v	0.1
N_{bat}	10^5	N_{pop}	50
N_{gen}	5.6×10^5		

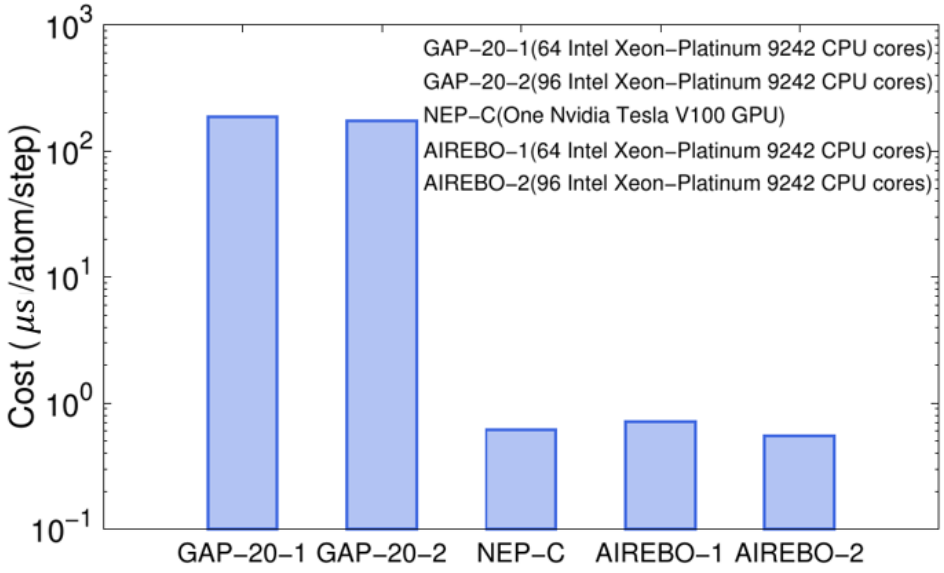

Fig. S1: The comparision of computational cost from NEP-C model with GAP-20 potential and AIREBO potential.

used. The NEP-C model is implemented on a GPU with an Nvidia V100 GPU, while the GAP-20 model and empirical potential AIREBO are parallelized by the message passing interface (MPI) using 64 and 96 Intel Xeon-Platinum 9242 CPU cores, respectively. Although the CPU and GPU resources may have unequal financial costs, one

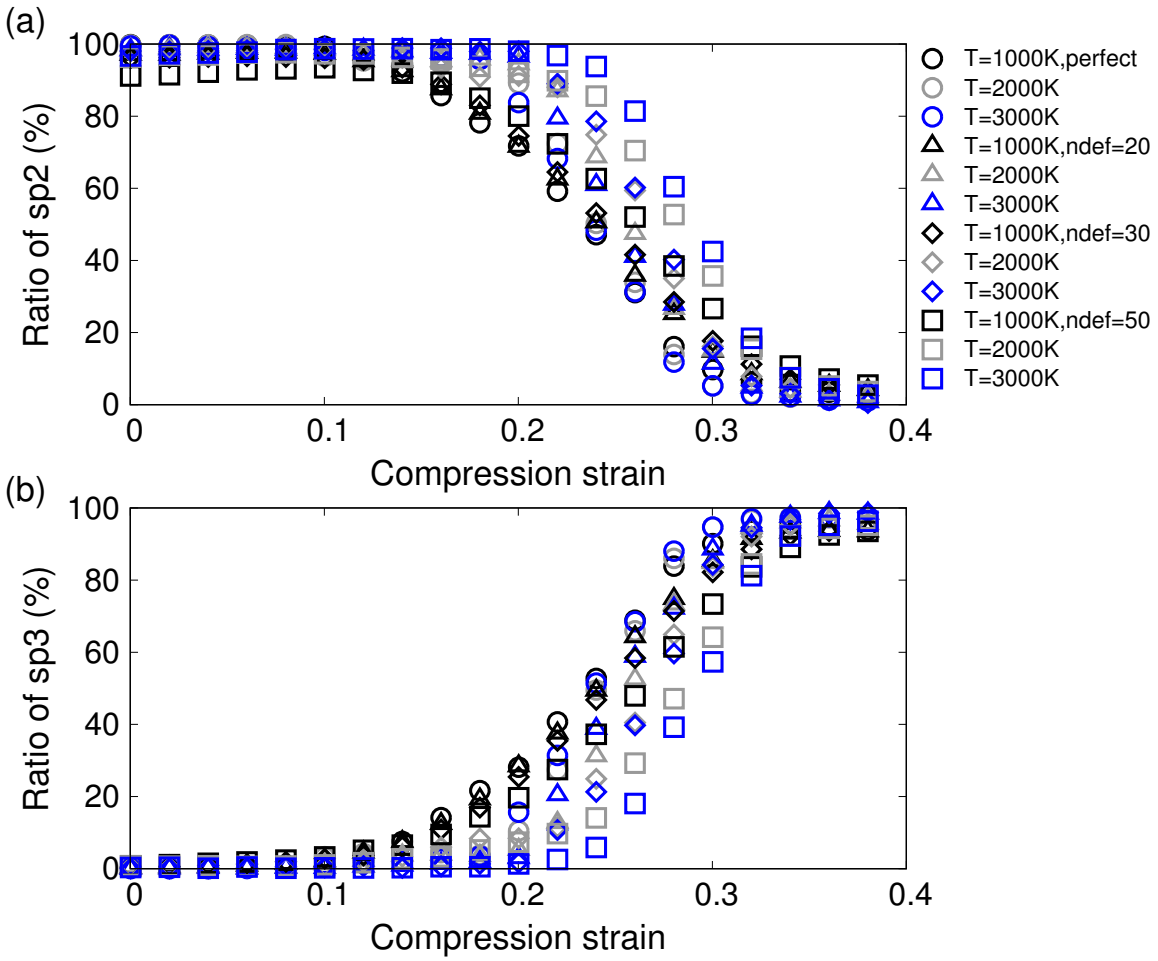

Fig. S2: The defect number effect on the ratio of (a) sp2- and (b) sp3- hybridized carbon atoms during the compression process at different temperatures.

can make suitable conversions of the results presented here to other computational environments. The results show that the computational speed of the GAP-20 potential is significantly slower by about three orders of magnitude than that of typical empirical potentials (AIREBO) on the same computing platform. However, the computational speed of the NEP-C model is comparable with the high-efficiency empirical potential AIREBO. This comparison highlights the superior computational performance of the NEP approach as implemented in GPUMD in terms of computational speed, which is crucial for large-scale and long time atomistic simulations.

Section 2

We investigate the correlation between the number of defects and the ratio of sp2- and sp3-hybridized carbon atoms in peapods, under different temperature and compressive strain conditions, as illustrated in Fig. S2. Notably, at elevated temperatures, peapods undergo a transformation into highly stable graphitic sheets under compres-

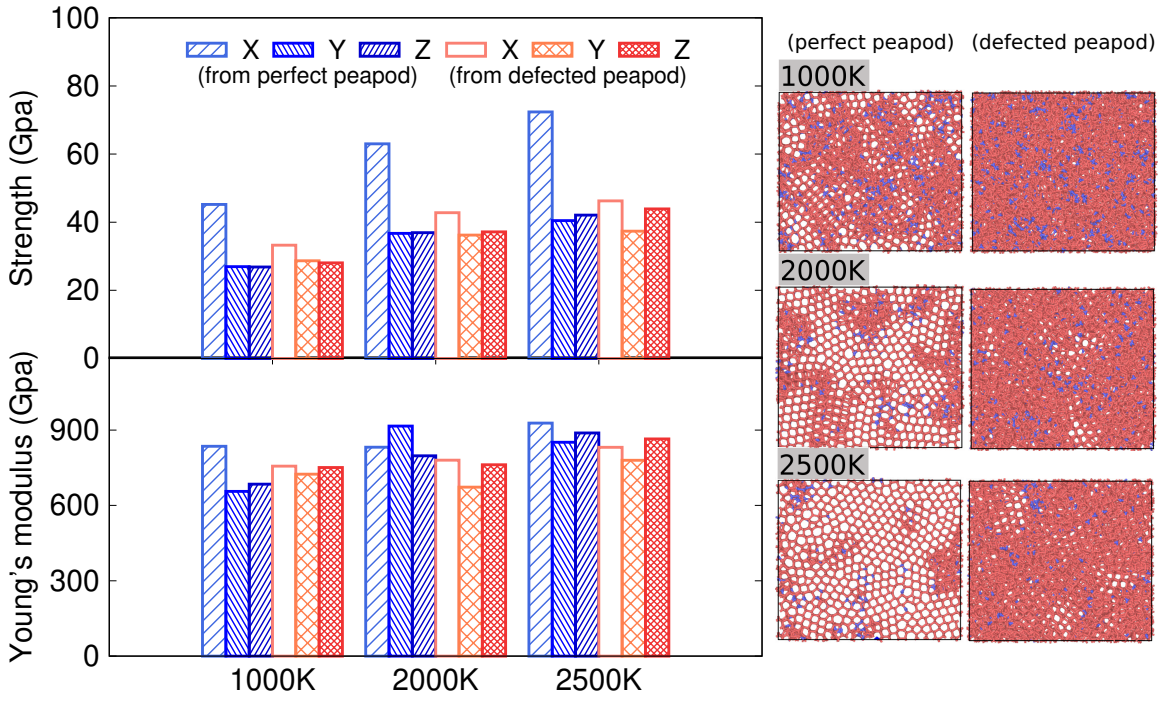

Fig. S3: Histograms of tensile strength and Young's modulus of structures obtained under substantial compressive strain.

sion. The lower density of the defected system introduces a greater inter-sheet spacing, which poses challenges to the transition from sp2- to sp3-hybridization. In contrast, the number of defects has minimal impact on the evolution of the sp2- and sp3-hybridized carbon atom ratio at lower temperatures.

Section 3

Figure S3 presents the structures obtained under a substantial compressive strain of 0.35, accompanied by their uniaxial tensile strength and Young's modulus. The perfect systems transform into sp3-hybridized diamond-rich structures, while the defected systems transform into sp3 amorphous carbon. Under greater compressive strain, the tensile strength and Young's modulus of defected systems are comparable to those of perfect systems, indicating that the highly compacted sp3 carbon materials possess superior mechanical strength and are suitable for use as hard and robust materials in numerous applications. The tensile strength of defected systems become nearly isotropic relative to perfect systems, with defects removing anisotropy in mechanical properties. Furthermore, the Young's modulus of both systems is almost isotropic. Stress–strain curves of the structures under uniaxial tension on the x, y and z directions, which obtained from the pefect and defected peapods under moderate and large compressive strain, are depicted in the Figs. S4 and S5.

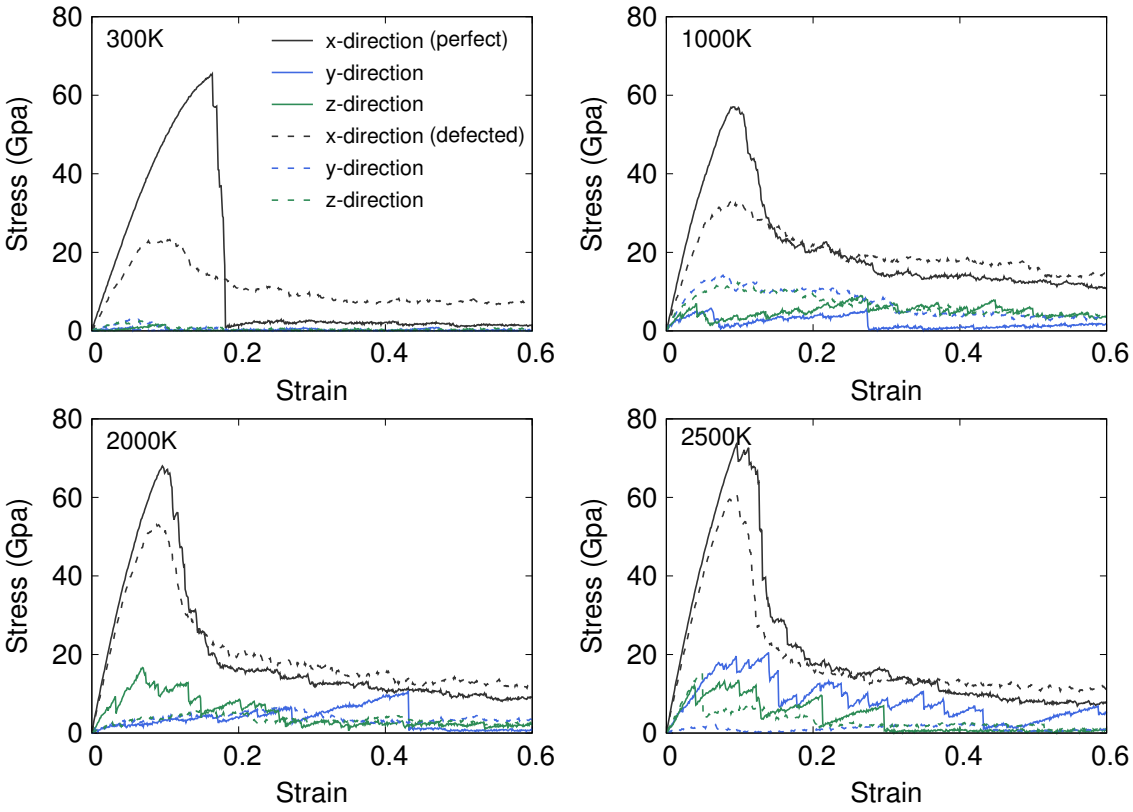

Fig. S4: Tensile stress–strain curves of the structures obtained from the pefect and defected peapods under moderate compressive strain.

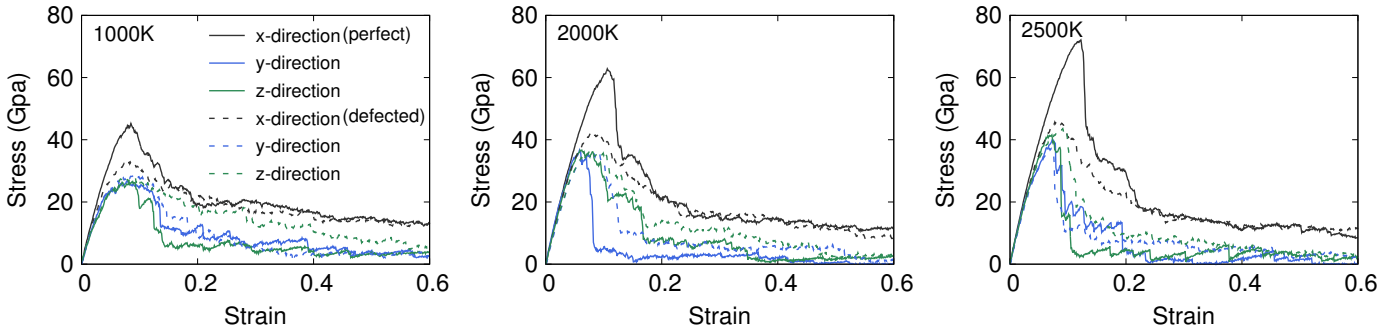

Fig. S5: Tensile stress–strain curves of the structures obtained from the pefect and defected peapods under large compressive strain.